

Ultrafast Two-Dimensional Infrared Spectroscopy Resolves the Conformational Change of an Evans Auxiliary Induced by $\text{Mg}(\text{ClO}_4)_2$

Andreas T. Messmer,¹ Sabrina Steinwand,¹ Katharina M. Lippert,[‡] Peter R. Schreiner,^{*,‡} and Jens Bredenbeck^{*,1,§}

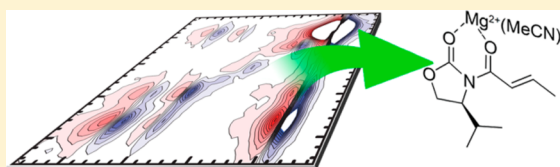
¹Institute of Biophysics, Johann Wolfgang von Goethe University, Max-von-Laue-Strasse 1, 60438 Frankfurt, Germany

[‡]Institute of Organic Chemistry, Justus-Liebig University, Heinrich-Buff-Ring 58, 35392 Giessen, Germany

[§]CEF-MC, Johann Wolfgang von Goethe University, Max-von-Laue-Strasse 9, 60438 Frankfurt, Germany

Supporting Information

ABSTRACT: Structure determination of reactive species is a key step in understanding reaction mechanisms. We demonstrate the application of polarization-dependent two-dimensional infrared spectroscopy (P2D-IR) as a powerful tool combining structure resolution with ultrafast time resolution. We apply this technique to investigate the substrate–catalyst complexes in a Lewis acid catalyzed Diels–Alder reaction. Using $\text{Mg}(\text{ClO}_4)_2$ as a Lewis acid, we found that an additional complex besides the chelate typically postulated as reactive species forms. Experimental access to this new species leads to a deeper understanding of the observed selectivities for the Diels–Alder reaction catalyzed by Lewis acids. Our findings are supported by density functional computations at the M06/6-31+G(*d,p*) level, including solvent corrections.



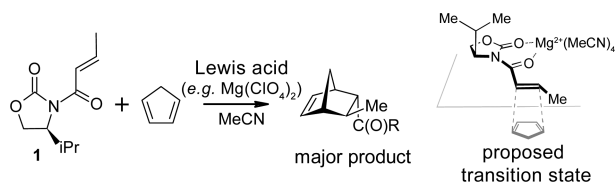
INTRODUCTION

One of the main challenges in modern chemistry is to develop new catalytic reactions and to optimize existing ones with respect to yield and selectivity. To cope with this task, it is essential to understand reaction mechanisms in detail and to determine the structures of the intermediates under the reaction conditions. Since most reactive intermediates are short-lived, otherwise extremely powerful tools like NMR are frequently not able to resolve their structures due to their low time resolution. Hence, complementary techniques for structure determination of short-lived species are highly desirable.

The reaction we focus on in this publication is the Lewis acid catalyzed, enantioselective Diels–Alder reaction of *N*-acyloxazolidin-2-one (**1**) with cyclopentadiene, a showcase example for stereocontrol using cation complexation introduced by Evans *et al.* (Scheme 1).¹ The selectivity of the reaction depends critically on controlling the conformation of the reactive species (the two carbonyl groups can be arranged antiperiplanar (*ap*) or synperiplanar (*sp*); the C–C single bond can be *s-cis* (*c*) or *s-trans* (*t*); the transition-state conformation

shown in Scheme 1 thus is termed *spc*).¹ To date, this reaction (with Et_2AlCl as Lewis acid) has become a textbook example to illustrate the power of chelation for controlling conformation as well as the use of chiral auxiliaries such as the chiral oxazolidinone used here, which is widely known as the Evans auxiliary.^{2,3} Although this and similar reactions are widely used, the reaction mechanism typically depicted in the literature is still mainly based on indirect evidence derived from the ensuing product stereochemistry. Santos *et al.* proposed an alternative mechanism, based on NMR studies, that does not involve a chelate but a bimetal complex as an important intermediate.⁴ NMR studies in the case of the Lewis acid SnCl_4 suggested the formation of a chelate.⁵ Only a single complex species was detected by NMR. The conformation of the crotonyl moiety was proposed to be *s-cis*, corresponding to the original proposal by Evans, however, without spectroscopic evidence. In a recent P2D-IR study, we resolved the *s-cis* conformer of the chelate as the major complex species, coexisting with a minor population of *s-trans*.⁶ This heterogeneity could be the cause of the low diastereoselectivity reported for the Lewis acid SnCl_4 .⁵ Uncomplexed **1** was determined to adopt the *apc* conformation. Here, we study the Lewis acid $\text{Mg}(\text{ClO}_4)_2$, which is frequently used in synthesis.^{7–10} It was found to form a chelate with **1**⁴ as well as with a very similar compound¹¹ in previous NMR studies using through-space magnetization transfer (nuclear Overhauser effect spectroscopy, NOESY). Based on the observed NOE cross peaks, the crotonyl conformation has been proposed to be *s-cis*. An equilibrium with the *s-trans*

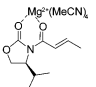
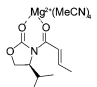
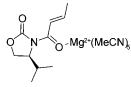
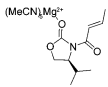
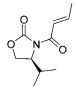
Scheme 1. Lewis Acid Catalyzed Diels–Alder Reaction and Proposed Transition State by Evans¹



Received: October 2, 2012

Published: November 30, 2012

Table 1. Comparison of the Experimental Data to the Computed (M06/6-31+G(d,p)/PCM/Bondi) Properties of Various **1**·Mg²⁺ Complexes in MeCN^a

		1-magnesium complexes					Free 1 ⁶	
		experiment					experiment	
		major species	1-spc-κ²O,O'	1-spt-κ²O,O'	1-apc-κO'	1-apc-κO		1-apc
Angle θ	ν_1/ν_2 (°)	36±3	35	43	67	58	61±2	61
	ν_1/ν_3 (°)	38±2	40	26	8	26	30±3	17
	ν_2/ν_3 (°)	64±2	74	35	64	32	47±3	45
wave-number	ν_1 (cm ⁻¹) ^b	1616	1615	1628	1622	1639	1639	1643
	ν_2 (cm ⁻¹) ^b	1650	1656	1664	1668	1693	1687	1687
	ν_3 (cm ⁻¹) ^b	1762	1759	1755	1785	1756	1776	1773

^aThe data for free **1** are shown in the last two columns. ^bAll computed vibrational wavenumbers of the magnesium complexes have been uniformly shifted by -51 cm⁻¹, the computed vibrational wavenumbers of **1** have been shifted by -47 cm⁻¹ (see the Supporting Information).

conformer has not been considered and would also be difficult or impossible to detect by NMR due to rapid exchange as shown in the case of the Lewis acid SnCl₄ by P2D-IR spectroscopy.⁶ Using this technique, we achieve subpicosecond time resolution that freezes out all isomerization processes and allows us to obtain direct conformational information by measuring vibrational transition dipole angles. In this way, we resolved the chelate **1-spc-κ²O,O'**·Mg²⁺(MeCN)₄ as the major species. In contrast to the chelation with SnCl₄, there is no indication for the presence of the *s-trans* conformer of the chelate in the case of Mg²⁺. Instead, the nonchelate species **1-apc-κO**·Mg²⁺(MeCN)₅ is likely to be present.

Polarization-dependent two-dimensional infrared (P2D-IR) spectroscopy has proven to be a powerful technique to determine the structure of small molecules in solution, especially under conditions where standard techniques like multidimensional NMR experiments have reached their limits.⁶ Similar to a 2D-NMR spectrum, the 2D-IR spectrum is spanned by two frequency axes and consists of diagonal and cross peaks.^{12–14} Cross peaks between vibrations occur if they interact with each other, i.e., couple. The relative cross peak intensities for different polarization conditions depend on the molecular structure, e.g., the angle between the transition dipole moments, as well as the polarization of the laser pulses used in the experiment. The signal dependence on the relative laser pulse polarization can be quantified by the anisotropy r calculated as

$$r(t) = \frac{\Delta\alpha_{\parallel}(t) - \Delta\alpha_{\perp}(t)}{\Delta\alpha_{\parallel}(t) + 2\Delta\alpha_{\perp}(t)} \quad (1)$$

where $\Delta\alpha_{\parallel}$ and $\Delta\alpha_{\perp}$ are the signal intensities for parallel and perpendicular polarization of pump and probe pulse.^{15,16} For a fixed isotropic distribution of molecules, the angle θ between two transition dipole moments can be determined using the relation

$$\theta = \cos^{-1} \sqrt{\frac{5r(t) + 1}{3}} \quad (2)$$

The anisotropy calculated with eq 2 can take values between 0.4 for parallel and -0.2 for perpendicular transition dipole

moments. As the molecules rotate on the time scale of the P2D-IR experiment, the anisotropy needs to be extrapolated to $t = 0$ ps in order to determine the transition dipole angles accurately.¹⁷

In the ideal case, where each stretching vibration is localized on one bond, the angle θ directly represents the molecular structure. However, usually the vibrations are delocalized and thus the transition dipole moments are not necessarily aligned with the bonds in the molecule. In these cases, quantum chemical computations give access to the orientation of the transition dipole moments for a given structure. The structure is deduced by comparison of computed and measured angles.

RESULTS AND DISCUSSION

Various structures for complexes between Lewis acidic metals and *N*-acyloxazolidinones have been discussed.^{1,4,5,18} To deduce the actual structure of the complex between **1** and Mg(ClO₄)₂ in MeCN from the transition dipole angles, we computed the vibrational frequencies as well as the transition dipole moments for a set of structures frequently referred to in the literature. The results are summarized in Table 1. Previous studies showed that Mg(ClO₄)₂ dissociates completely in MeCN and the Mg²⁺ ion is, at low concentrations, hexacoordinated by the solvent.¹⁹ Hence, we looked only at complexes between Mg²⁺ and **1**, in which the remaining coordination sites were occupied by MeCN.

The FTIR spectrum of the mixture of **1** and Mg(ClO₄)₂ in MeCN (Figure 1a) shows three main signals ($\nu_1 = 1616$ cm⁻¹, $\nu_2 = 1650$ cm⁻¹, and $\nu_3 = 1762$ cm⁻¹) originating from the carbonyl and alkenyl stretching vibrations (cf. Scheme 1 for the structure). All three bands shift to lower wavenumber upon complexation compared to free **1** (Table 1). The computed wavenumbers for the chelate structures **1-spc-κ²O,O'**·Mg²⁺(MeCN)₄ and **1-spt-κ²O,O'**·Mg²⁺(MeCN)₄ agree well with the experimental wavenumbers (Table 1). A clear-cut discrimination between the two is achieved by P2D-IR spectroscopy, as shown below. The band origins computed for the species with monodentate complexation **1-apc-κO'**·Mg²⁺(MeCN)₅ and **1-apc-κO**·Mg²⁺(MeCN)₅ do not match the main bands in the FTIR spectrum well, as either ν_2 or ν_3 is too high compared to the experimental value,

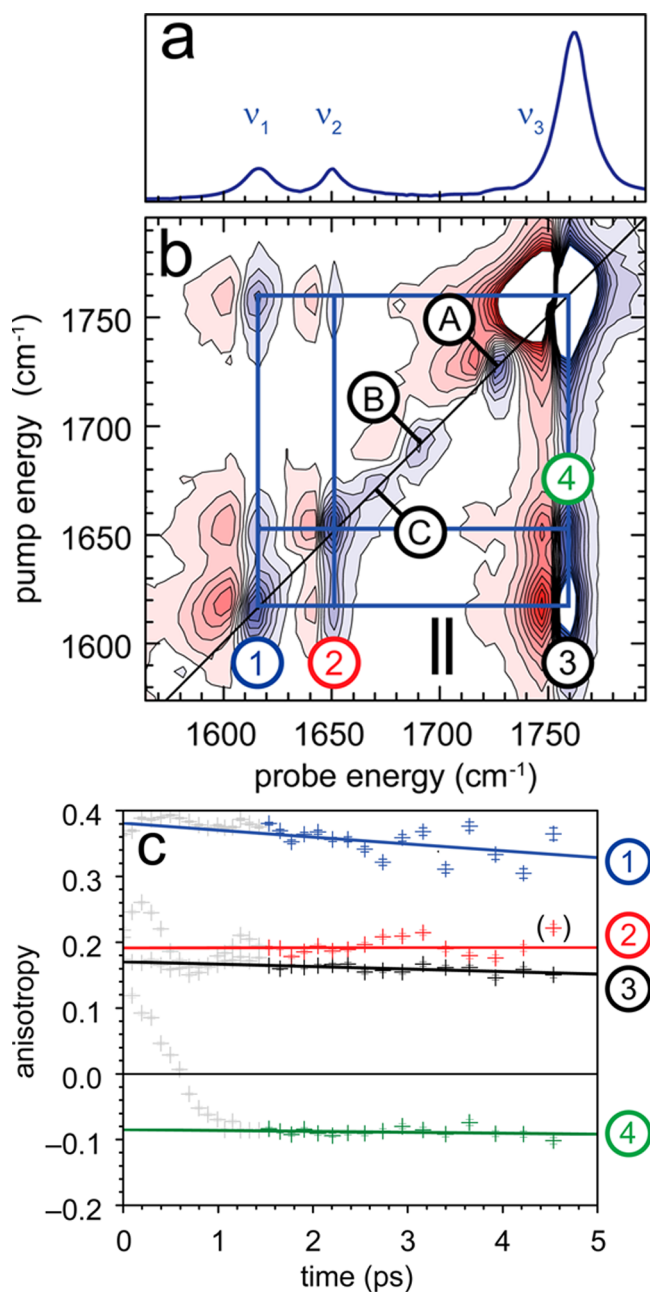


Figure 1. (a) FTIR spectrum of a solution of **1** (34 mM) and $\text{Mg}(\text{ClO}_4)_2$ (0.38 M) in MeCN. (b) Corresponding P2D-IR spectrum (1.5 ps, 10 °C, parallel polarization). The contour lines are spaced by 0.05 mOD. Signals larger than ± 0.5 mOD are truncated. (c) Time dependence of the anisotropy for the signals marked in (b). The straight lines show the linear fit of the data from 1.5 to 5 ps. The data point in parentheses is omitted for the analysis (see the Supporting Information). The data points with a delay of less than 1.5 ps are shown in gray.

depending on whether the crotonyl oxygen or the ring oxygen interacts with the Lewis acid.

More detailed structure information and higher sensitivity for minor species is available from P2D-IR spectroscopy. The P2D-IR spectrum of the carbonyl and alkenyl stretching vibrations (Figure 1b) is dominated by three diagonal peaks corresponding to the signals seen in the FTIR spectrum and the cross peaks between them (highlighted by the blue grid). The time-dependent anisotropy of the numbered signals required to

determine the transition dipole angles is shown in Figure 1c. The data with a delay time between 1.5 and 5 ps were linearly extrapolated (straight lines) to determine the initial anisotropies. For the rotational diffusion times observed here, a linear fit in this time range is sufficient for precise angle determination.⁶ For the diagonal peak of ν_1 (blue, position 1), the anisotropy extrapolated to 0.38(2), which is in good agreement with the value of 0.4 expected for a diagonal peak. For a diagonal peak, the pump and probe pulse are interacting with the same transition dipole, and hence, the value for parallel transition dipoles is obtained. The cross peak between ν_1 and ν_2 (red, position 2) showed an initial anisotropy of 0.191(10). Using eq 2, this translates into an angle θ of $36^\circ \pm 3^\circ$. The error of 3° includes experimental errors as well as the standard deviation of the linear fit. The extrapolation of the time dependent anisotropy for the cross peaks between ν_1 and ν_3 (black, position 3) and ν_2 and ν_3 (green, position 4) results in angles of $38 \pm 2^\circ$ and $64 \pm 2^\circ$, respectively.

The computed angles of $\mathbf{1}\text{-spc-}\kappa^2\text{O, O}'\cdot\text{Mg}^{2+}(\text{MeCN})_4$ match the experiment very well. In addition, the computed vibrational band origins match nicely. On the other hand, the angles of all other computed species deviate strongly from the measurements. The comparison of the angles resulted in a deviation of up to 32° for the angle between ν_2 and ν_3 for the complex $\mathbf{1}\text{-apc-}\kappa\text{O}\cdot\text{Mg}^{2+}(\text{MeCN})_5$; the corrected vibrational frequencies deviated up to 43 cm^{-1} for ν_2 in this conformer. The comparison therefore led to the conclusion that the major species formed is the chelate $\mathbf{1}\text{-spc-}\kappa^2\text{O, O}'\cdot\text{Mg}^{2+}(\text{MeCN})_4$.

In addition to the signals analyzed so far (originating from the major species) we see additional, weaker signals (Figure 1b, positions A–C). These could potentially belong to additional complexes formed between **1** and Mg^{2+} in MeCN. Since such complexes could result in side products, i.e., other stereoisomers, knowledge about these species is a prerequisite to understand the observed stereoselectivity of the Lewis acid catalyzed Diels–Alder reactions. We will therefore discuss these minor signals in the following.

The signal at position A (Figure 1b) is shifted by $\sim 37\text{ cm}^{-1}$ from the ν_3 band and is caused by a ^{13}C isotopologue (see the Supporting Information).

The diagonal band at position B (Figure 1b) is located at $\sim 1690\text{ cm}^{-1}$. Zooming into the P2D-IR spectrum (Figure 2), weak cross peaks to a band at $\sim 1645\text{ cm}^{-1}$ appear (Figure 2, position I below the diagonal, position I' above the diagonal). The position of the cross peaks is indicated by the dashed ellipses. In a 2D-IR spectrum, each peak consists of a negative (blue) and a positive (red) part. However, because of the small signal size, the red part of the cross peak I is canceled by the nearby diagonal peak, whereas for cross peak I' the blue part is almost canceled (see the Supporting Information for cross-sections through the cross peaks). The positions of the two bands connected by the cross peaks ($\sim 1645\text{ cm}^{-1}$ and $\sim 1690\text{ cm}^{-1}$) fit well to the cross peaks ($\sim 1645\text{ cm}^{-1}$ and $\sim 1690\text{ cm}^{-1}$) as well as to the bands observed for uncomplexed **1** ($\nu_1 = 1639\text{ cm}^{-1}$ and $\nu_2 = 1687\text{ cm}^{-1}$). Also based on the polarization dependence of the cross peak between the two bands, the two species cannot be discriminated since the angles between the transition dipole moments of the involved vibrations are very similar (61° for **1** and 58° for $\mathbf{1}\text{-apc-}\kappa\text{O}\cdot\text{Mg}^{2+}(\text{MeCN})_5$). Observation of cross peaks from the bands at $\sim 1690\text{ cm}^{-1}$ and $\sim 1645\text{ cm}^{-1}$ to the respective band ν_3 would allow assignment of these two bands to uncomplexed **1** or $\mathbf{1}\text{-apc-}$

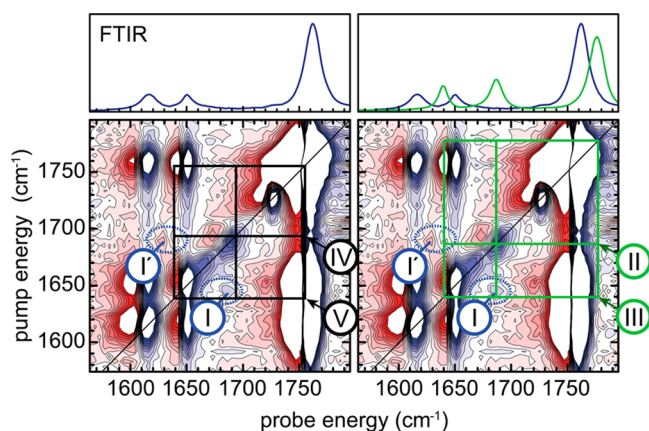


Figure 2. P2D-IR spectrum of **1** (34 mM) and $\text{Mg}(\text{ClO}_4)_2$ (0.38 M) in MeCN (1.5 ps, perpendicular polarization). The contour lines are spaced by $6 \mu\text{OD}$. Signals larger than $\pm 0.06 \text{ mOD}$ are truncated. The FTIR spectrum is shown in the top panel for orientation (blue: mixture of **1** and $\text{Mg}(\text{ClO}_4)_2$; green: free **1**, 34 mM in MeCN). The grid for **1-apc-κO·Mg²⁺(MeCN)₅** (black) is based on the DFT computations (Table 1), while the grid for the coupling pattern for free **1** (green) is based on experimental data. The points labeled by roman numerals are discussed in the text. For the spectrum with parallel polarization as well as selected cross-sections through the spectra, see the Supporting Information.

$\kappa\text{O·Mg}^{2+}(\text{MeCN})_5$ since the cross peaks expected for the two species differ considerably in frequency as well as in anisotropy. To assess the presence of cross-peaks with ν_3 , the observed coupling pattern for **1**⁶ and the computed pattern for **1-apc-κO·Mg²⁺(MeCN)₅** are plotted in Figure 2 (**1**: green grid, **1-apc-κO·Mg²⁺(MeCN)₅**: black grid). This plot illustrates that the weak cross peaks that might occur overlap with the strong signals from the major species.

If the observed signals at $\sim 1690 \text{ cm}^{-1}$ and $\sim 1645 \text{ cm}^{-1}$ were caused by free **1**, the cross peaks should appear on the high energy side of the bands of the major species (Figure 2, positions II and III). They are expected to be approximately three contour lines large in the spectrum shown in Figure 2, but they are absent. Also, we do not observe a diagonal peak of ν_3 for **1**. This leads to the conclusion that the signals are not caused by free **1**. However, it should be noted that due to the overlapping bands and the signal-to-noise ratio of the spectra the presence of the cross peaks for free **1** cannot be entirely excluded.

In the case that the complex **1-apc-κO·Mg²⁺(MeCN)₅** was responsible for the observed signals, the cross peaks with the high energy vibration would be slightly red-shifted compared to the major species. The bleach part of these cross peaks would, in probe direction, lie directly between the negative and positive part of the cross peak of the major species (Figure 2, positions IV and V). Because of the steep line shape of the cross peaks from the major species, weak cross peaks unfortunately cannot be detected in this region. The cross peaks at positions II and IV are sitting on top of the shoulder of both the diagonal peak ν_3 and the cross peak ν_2/ν_3 of the major species. In order to assign potential peaks at positions II and IV unambiguously, experiments with a higher resolution in pump direction are required. Sufficient resolution might be realized by using a pulse pair instead of a narrowband Fabry–Perot pump pulse.^{20–22}

There is a third diagonal peak not caused by the major species arising at $\sim 1670 \text{ cm}^{-1}$ (Figure 1, position C). This

signal is likely due to small amounts of water in the sample. If the sample is prepared with dry reagents but in absence of molecular sieve, we observe a broad band at 1670 cm^{-1} that grows with time. This band is strongly reduced but not suppressed completely, when molecular sieve is added to the solution, as has been done in the sample preparation for the measurements presented here. Alternatively, this signal could be explained the chelate **1-spt-κ²O,O'·Mg²⁺(MeCN)₄** ($\nu_2 = 1664 \text{ cm}^{-1}$), which, however, is computed to be $5.2 \text{ kcal mol}^{-1}$ higher in energy than the major species, **1-spc-κ²O,O'·Mg²⁺(MeCN)₄**. The presence of the chelate **1-spt-κ²O,O'·Mg²⁺(MeCN)₄** has been suggested for complexes of **1** with SnCl_4 .^{5,6}

CONCLUSION

In conclusion, by measuring the angles between the transition dipole moments of specific vibrations with P2D-IR, we provide strong evidence that **1** changes its conformation upon addition of the Lewis acid $\text{Mg}(\text{ClO}_4)_2$ and mainly forms the chelate **1-spc-κ²O,O'·Mg²⁺(MeCN)₄**. This finding is in agreement with previous NMR and quantum chemical studies. Due to the higher time resolution in combination with the higher sensitivity, one additional species in solution was detected, giving rise to diagonal peak B and cross peaks I and I', that suggest the presence of **1-apc-κO·Mg²⁺(MeCN)₅** which was not observed in earlier NMR experiments. The absence of these signals is mainly caused by motional averaging and therefore an inherent limitation in NMR. In order to assign the additionally detected species unambiguously to a complex structure, experiments with higher frequency resolution would be desirable. In the case of the Lewis acid SnCl_4 , an additional chelate with *s-trans* orientation of the crotonyl moiety (**1-spt-κ²O,O'**) has been detected.⁶ For Mg^{2+} , we did not observe this additional chelate.

As shown here, P2D-IR spectroscopy is a powerful tool for identifying catalyst–substrate complexes. Its high sensitivity in combination with femtosecond time resolution opens the possibility to investigate short-lived, reactive complexes at low concentrations. More detailed knowledge about such intermediates will have significant impact on understanding reaction mechanisms in detail as well as on the design of new catalysts with higher selectivities and activities.

EXPERIMENTAL SECTION

Sample Preparation. Compound **1** was synthesized following the procedures described in the literature.^{1,2,3} Commercial, dry $\text{Mg}(\text{ClO}_4)_2$ was dried further for 4 h at $104 \text{ }^\circ\text{C}$ and 10^{-3} mbar prior to use. For the P2D-IR measurements 4.4 mg of **1** and 55.8 mg of dry $\text{Mg}(\text{ClO}_4)_2$ were dissolved in 660 μL of dry acetonitrile (MeCN). The solution was stirred with molecular sieve for 12 h to remove residual water.

P2D-IR Spectroscopy. The P2D-IR setup used is described in detail in ref 3. In brief, the output of a Ti:sapphire-oscillator/amplifier system (Spectra Physics, Spitfire XP, 800 nm, 120 fs, 1 kHz) was used to generate mid-IR pulses ($\sim 2.4 \mu\text{J}/\text{pulse}$, center frequency around 1660 cm^{-1} , bandwidth $\sim 200 \text{ cm}^{-1}$ fwhm, pulse length $\sim 150 \text{ fs}$) in a two stage optical parametric amplifier.^{6,24} In the subsequent pump–probe P2D-IR setup based on the concept of Hamm et al., the mid-IR pulses were split into a pump, a probe, and a reference beam.²⁵ The pump beam passed a computer-controlled Fabry–Perot filter and was moved in time by a computer-controlled delay line. Pump and probe beam are focused with an off axis parabolic mirror in spatial overlap into the sample cell with an optical path length of 250 μm .²⁶ The sample cell was kept at $10 \text{ }^\circ\text{C}$. Special care was taken to obtain proper polarizations of the beams at the sample position. The polarization of the chopped pump beam was rotated by 45° relative to probe and

reference polarization.^{17,27,28} The polarization contrast at the sample position was >1400:1 for the pump and >1200:1 for probe and reference. Probe and reference beam passed directly after the sample through a motorized, computer controlled polarizer, while the pump beam was blocked. The motorized polarizer swapped every 300 laser shots between +45° and -45° relative to the probe polarization and therefore allowed a quasi simultaneous measurement of parallel and perpendicular polarization. After collimating both beams, they were frequency dispersed by a spectrometer onto a 2 × 32 pixel mercury–cadmium-telluride detector array.

The P2D-IR signal was calculated as the difference of absorption between the pumped and unpumped sample. All spectra were measured in four blocks directly after each other to span the whole region of interest, with minimal changes to the setup. Subsequently, the blocks were set together to the final spectrum without further treatment.

Computational Details. All computations were performed employing the Gaussian09 program suite,²⁹ using density functional theory (DFT) with Truhlar's hybrid meta-exchange-correlation functional M06³⁰ in conjunction with the 6-31+G(d,p) basis set.⁶ All structures were identified as minima by computing vibrational frequencies (only real frequencies were found). The influence of the solvent was taken into account by the self-consistent reaction field (SCRF) method, employing the polarizable continuum model (PCM)³¹ with van der Waals radii of Bondi³² with the Gaussian09 default scaling of 1.1 and explicit hydrogen atoms. Transition dipole moments were obtained from the frequency computations, and their relative angles were calculated from them.

■ ASSOCIATED CONTENT

■ Supporting Information

P2D-IR spectra with both polarizations; alternative fit of the data shown in Figure 1c; positions of isotopologue signals; selected cross-sections through P2D-IR spectra of Figure 2. This material is available free of charge via the Internet at <http://pubs.acs.org>.

■ AUTHOR INFORMATION

Corresponding Author

*E-mail: (J.B.) bredenbeck@biophysik.uni-frankfurt.de, (P.R.S.) prs@org.chemie.uni-giessen.de.

Notes

The authors declare no competing financial interest.

■ ACKNOWLEDGMENTS

A.T.M. thanks the Fonds der chemischen Industrie (FCI) for a Kekulé fellowship. J.B. gratefully acknowledges funding by the Alexander von Humboldt Foundation through a Sofja Kovalevskaja award. We thank J. Glatthaar for the purification of Mg(ClO₄)₂ and helpful discussions.

■ REFERENCES

- (1) Evans, D. A.; Chapman, K. T.; Bisaha, J. *J. Am. Chem. Soc.* **1988**, *110*, 1238–1256.
- (2) Clayden, J.; Greeves, N.; Warren, S.; Wothers, P. *Organic Chemistry*; Oxford University Press: Oxford, 2001.
- (3) Gnas, Y.; Glorius, F. *Synthesis* **2006**, *12*, 1899–1930.
- (4) Bakalova, S. M.; Duarte, F. J. S.; Georgieva, M. K.; Cabrita, E. J.; Santos, A. G. *Chem.—Eur. J.* **2009**, *15*, 7665–7677.
- (5) Castellino, S. *J. Org. Chem.* **1990**, *55*, 5197–5200.
- (6) Messmer, A. T.; Lippert, K. M.; Steinwand, S.; Lerch, E.-B. W.; Hof, K.; Ley, D.; Gerbig, D.; Hausmann, H.; Schreiner, P. R.; Bredenbeck, J. *Chem.—Eur. J.* **2012**, *18*, 14989–14995.
- (7) Tomioka, K.; Muraoka, A.; Kanai, M. *J. Org. Chem.* **1995**, *60*, 6188–6190.
- (8) Adam, W.; Zhang, A. *Eur. J. Org. Chem.* **2004**, 147–152.

- (9) Dugović, B.; Fišera, L.; Hametner, C. *Synlett* **2004**, 1569–1572.
- (10) Desimoni, G.; Faita, G.; Invernizzi, A. G.; Righetti, P. *Tetrahedron* **1997**, *53*, 7671–7688.
- (11) Kanai, M.; Muraoka, A.; Tanaka, T.; Sawada, M.; Ikota, N.; Tomioka, K. *Tetrahedron Lett.* **1995**, *36*, 9349–9352.
- (12) Cho, M. *Chem. Rev.* **2008**, *108*, 1331–1418.
- (13) Woutersen, S.; Hamm, P. *J. Phys.: Condens. Matter* **2002**, *14*, R1035–R1062.
- (14) Zanni, M. T.; Hochstrasser, R. M. *Curr. Opin. Struct. Biol.* **2001**, *11*, 516–522.
- (15) Andrews, S. S. *J. Chem. Educ.* **2004**, *81*, 877–885.
- (16) Berne, B. J.; Pecora, R. *Dynamic Light Scattering: With Applications to Chemistry, Biology, and Physics*; Dover Publication: Dover, 2000.
- (17) Rezus, Y. L. A.; Bakker, H. J. *Proc. Natl. Acad. Sci. U.S.A.* **2006**, *103*, 18417–18420.
- (18) Castellino, S.; Dwight, W. J. *J. Am. Chem. Soc.* **1993**, *115*, 2986–2987.
- (19) Cha, J.-N.; Cheong, B.-S.; Cho, H.-G. *J. Phys. Chem. A* **2011**, *105*, 1789–1796.
- (20) DeFlores, L. P.; Nicodemus, R. A.; Tokmakoff, A. *Opt. Lett.* **2007**, *32*, 2966–2968.
- (21) Helbing, J.; Hamm, P. *J. Opt. Soc. Am. B* **2011**, *28*, 171–178.
- (22) Shim, S.-H.; Strasfeld, D. B.; Ling, Y. L.; Zanni, M. T. *Proc. Natl. Acad. Sci. U.S.A.* **2007**, *104*, 14197–14202.
- (23) Benoit, D.; Coulbeck, E.; Eames, J.; Motevalli, M. *Tetrahedron: Asymmetry* **2008**, *19*, 1068–1077.
- (24) Hamm, P.; Kaindl, R. A.; Stenger, J. *Opt. Lett.* **2000**, *25*, 1798–1800.
- (25) Hamm, P.; Lim, M.; Hochstrasser, R. M. *J. Phys. Chem. B* **1998**, *102*, 6123–6138.
- (26) Bredenbeck, J.; Hamm, P. *Rev. Sci. Instrum.* **2003**, *74*, 3188.
- (27) Graener, H.; Seifert, G.; Laubereau, A. *Chem. Phys. Lett.* **1990**, *172*, 435–439.
- (28) Ramasesha, K.; Roberts, S. T.; Nicodemus, R. A.; Mandal, A.; Tokmakoff, A. *J. Chem. Phys.* **2011**, *135*, 054509.
- (29) Frisch, M. J.; Trucks, G. W.; Cheeseman, J. R.; Scalmani, G.; Caricato, M.; Hratchian, H. P.; Li, X.; Barone, V.; Bloino, J.; Zheng, G.; Vreven, T.; Montgomery, J. A.; Petersson, G. A.; Scuseria, G. E.; Schlegel, H. B.; Nakatsuji, H.; Izmaylov, A. F.; Martin, R. L.; Sonnenberg, J. L.; Peralta, J. E.; Heyd, J. J.; Brothers, E.; Ogliaro, F.; Bearpark, M.; Robb, M. A.; Mennucci, B.; Kudin, K. N.; Staroverov, V. N.; Kobayashi, R.; Normand, J.; Rendell, A.; Gomperts, R.; Zakrzewski, V. G.; Hada, M.; Ehara, M.; Toyota, K.; Fukuda, R.; Hasegawa, J.; Ishida, M.; Nakajima, T.; Honda, Y.; Kitao, O.; Nakai, H.; Vreven, T.; Montgomery, J. A., Jr.; Peralta, J. E.; Ogliaro, F.; Bearpark, M.; Heyd, J. J.; Brothers, E.; Kudin, K. N.; Staroverov, V. N.; Kobayashi, R.; Normand, J.; Raghavachari, K.; Rendell, A.; Burant, J. C.; Iyengar, S. S.; Tomasi, J.; Cossi, M.; Rega, N.; Millam, J. M.; Klene, M.; Knox, J. E.; Cross, J. B.; Bakken, V.; Adamo, C.; Jaramillo, J.; Gomperts, R.; Stratmann, R. E.; Yazyev, O.; Austin, A. J.; Cammi, R.; Pomelli, C.; Ochterski, J. W.; Martin, R. L.; Morokuma, K.; Zakrzewski, V. G.; Voth, G. A.; Salvador, P.; Dannenberg, J. J.; Dapprich, S.; Daniels, A. D.; Farkas, Ö.; Foresman, J. B.; Ortiz, J. V.; Cioslowski, J.; Fox, D. J. *Gaussian 09 Revision B.01*; Gaussian, Inc.: Wallingford, CT, 2009.
- (30) Zhao, Y.; Truhlar, D. G. *Theor. Chem. Acc.* **2008**, *120*, 215–241.
- (31) Tomasi, J.; Mennucci, B.; Cammi, R. *Chem. Rev.* **2005**, *105*, 2999–3094.
- (32) Bondi, A. *J. Phys. Chem.* **1964**, *68*, 441–451.